THE ATLANTIC-WIDE RESEARCH PROGRAMME FOR BLUEFIN TUNA

(GBYP Phase 10)

SHORT TERM CONTRACT FOR BFT GROWTH IN FARMS

PILOT STUDY

(ICCAT GBYP 10/2020)

Final Report (Deliverable 7)

Valencia, 26 July 2021

Universitat Politècnica de València

This project is co-funded by
the European Union

Signed by VICTOR ESPINOSA ROSELLO - NIF:00810150K on the 24/08/2021 with a certificate emitted by ACCVCA-120

BFT Growth in Farms Pilot Study (ICCAT GBYP 10/2020)

P. Muñoz-Benavent[1], V. Puig-Pons[2], A. Morillo-Faro [2], G. Andreu-García[1], V. Espinosa[2], I. Pérez-Arjona[2]

SUMMARY

The present work describes the results obtained with an autonomous monitoring system installed from 28th July 2020 to 23rd May 2021 in a fattening cage in Grup Balfegó (West Mediterranean) containing 724 BFT. The system is able to provide thousands of accurate automatic measurements per day, so the evolution of tuna sizes can be studied in detail thanks to such a great amount of information. Regarding the tuna length and width, the results suggest that from September 2020 to May 2021 the growth in length is approximately between 8 and 18 cm (between 3% and 10%) and the growth in maximum width between 1.2 and 3.0 centimeters (between 2% and 10%), depending on the fish length. The acoustic system is also used to estimate the height of the fish to provide a more accurate biomass estimation. Different expressions deduced from slaughtered fish are proposed based on formulae relating weight and dimensions (length, width and height) of Bluefin tuna fattened in captivity. The results confirm that the availability of more than one dimension reduces error in the estimate.

KEYWORDS

Stereoscopic computer vision, acoustics, biomass estimation

[1] {pmunyoz,gandreu}@upv.es. Institute of Control Systems and Industrial Computing (AI2). Universitat Politècnica de València (UPV).

[2] {vipuipon, anmofa, vespinos, iparjona}@upv.es Institut d'Investigació per a la Gestió Integrada de Zones Costaneres (IGIC). Universitat Politècnica de València (UPV).

Introduction

This work constitutes the sixth deliverable ("Draft final report") agreed in the amendment to the contract between ICCAT and UPV, consisting in a scientific report describing in detail the work carried out and the obtained results, including:

a) Evolution of length, width and height distributions estimated with the UPV automatic software on a daily basis, as long as the environmental conditions, fish behaviour and system integrity allow us to gather enough information in each daily session. Otherwise, the UPV shall define the optimal reporting intervals.

b) Evolution of total biomass estimated using only acoustic sensors by monitoring the acoustical target strength.

c) Statistical analyses determining the influence of food supply and environmental variables on the estimated fish growth, both in weight and length, along the studies period.

d) Viability of automatic BFT biometric measurements in air during harvesting.

e) This draft Final Report will include also an Executive Summary.

The monitoring period established initially from July 2020 to December 2020 was finally modified due to market needs of Grup Balfegó. The fish were finally harvested in July 2021 and the study was extended until that date to avoid the temporal mismatch between optical and acoustical measurements and BFT biometrics obtained from slaughtered fish (ground truth data).

1. Data and methods

1.1 Description of the system

The cage is cylinder-shaped with a base of 50 m of diameter in the water surface and 35 m high in its lowest point, which is an approximate volume of 20,000 m3. The system is composed of a subsea sensors platform, which is positioned on the bottom of the cage (23 meters depth), and a logging subsystem, which is tied to the cage structure in the surface. An overview of the system can be observed in Figure 1.

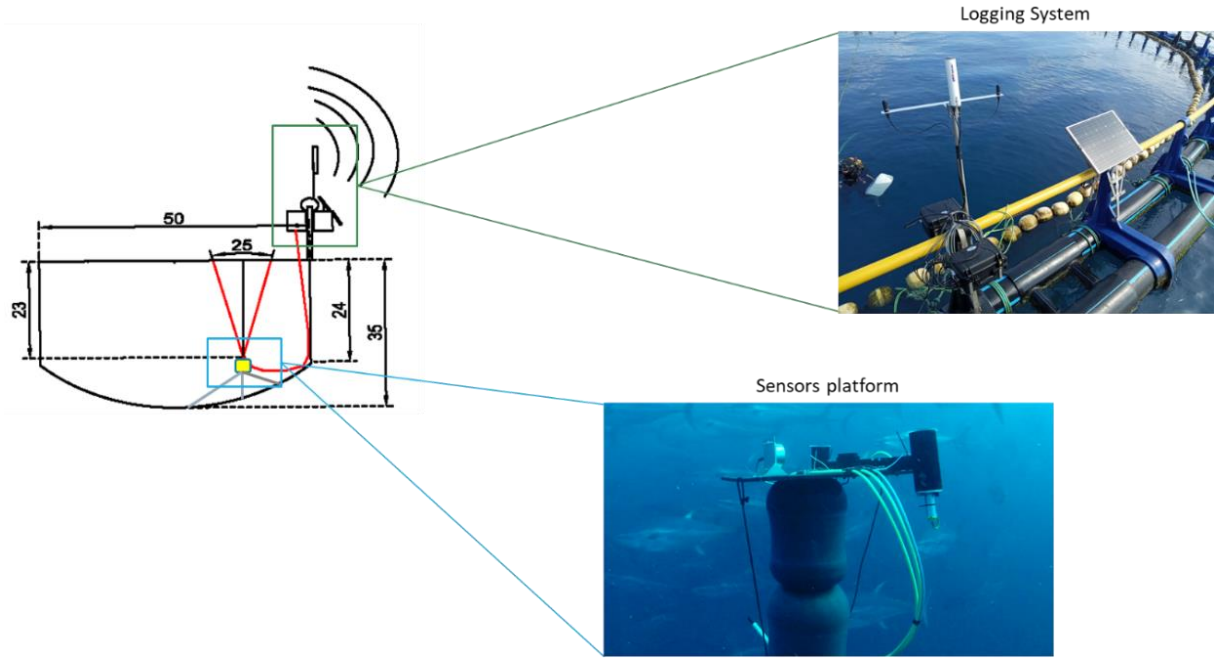

Figure 1. Overview of the parts of the system

1.1.1. Subsea Sensors Platform

The sensors platform was equipped with a stereoscopic camera, an inclinometer and a 120 kHz single beam transducer. It was positioned lying on the bottom of the cage and looking towards the surface in order to have a ventral perspective of the fish. Buoys gives the platform positive buoyancy and ropes tie the platform to the cage. Figure 2 shows an image of a sensors platform installed in the Grup Balfegó facilities.

The 120 kHz single-beam transducer (Airmar depth transducer 190947-02) operated by a Zunibal ZSR-Aqua echosounder was set up with a transmitting power of 50 W, pulse length of 150 µs and 4 pings per second. The nominal acoustic beam angle was 11.1°. The on-axis and off-axis calibration was carried out using the standard calibration method, with a 38.1 mm diameter tungsten-carbide sphere.

Video recordings were taken with a customized stereo camera comprised of two Gigabit Ethernet cameras, with a 2048 x 1536 pixel (3.1 Megapixels) resolution and framerate of 20 fps. The cameras were mounted in an underwater housing, with a baseline of 85 cm and inward convergence of 5°. Camera synchronization was achieved using the IEEE 1588 Precision Time Protocol (PTP). The system is rated for a depth of 40 m and has an umbilical cable that supplies power over Ethernet to the cameras and transfers images to a logging computer, which encodes left and right videos using hardware encoding. The stereoscopic system was previously calibrated using a checkerboard pattern and the MATLAB® Stereo Calibration Application.

Two UPV systems with different focal lengths have been used. A system with 12,5 mm focal length lenses was initially installed. During the first months we realized that the water turbidity conditions were extremely worse than previously observed in l'Ametlla de Mar and most of the days tuna could not be measured in the whole column range. With the 12,5 mm focal length lenses, fish can be measured at distances starting from 6 meters, because they cannot fit completely into the field of view at lower distances. Thus, we decided to replace the system and install another one with 6 mm focal length lenses, which allows sizing the fish at distances starting

from 3 meters.

Moreover, some recordings were taken using the AM100 stereovision system (www.aq1systems.com). It uses two Gigabit Ethernet cameras, with image resolution of 1360x1024 pixels, 3.5 mm focal length lenses and framerate of 12 fps. The cameras are mounted in an underwater housing, with a baseline of 80cm and an inward convergence of 6º. The system is rated to 40m deep and has an umbilical cable that supplies power to the cameras and transfers images to a logging computer, which generates synchronized left and right videos.

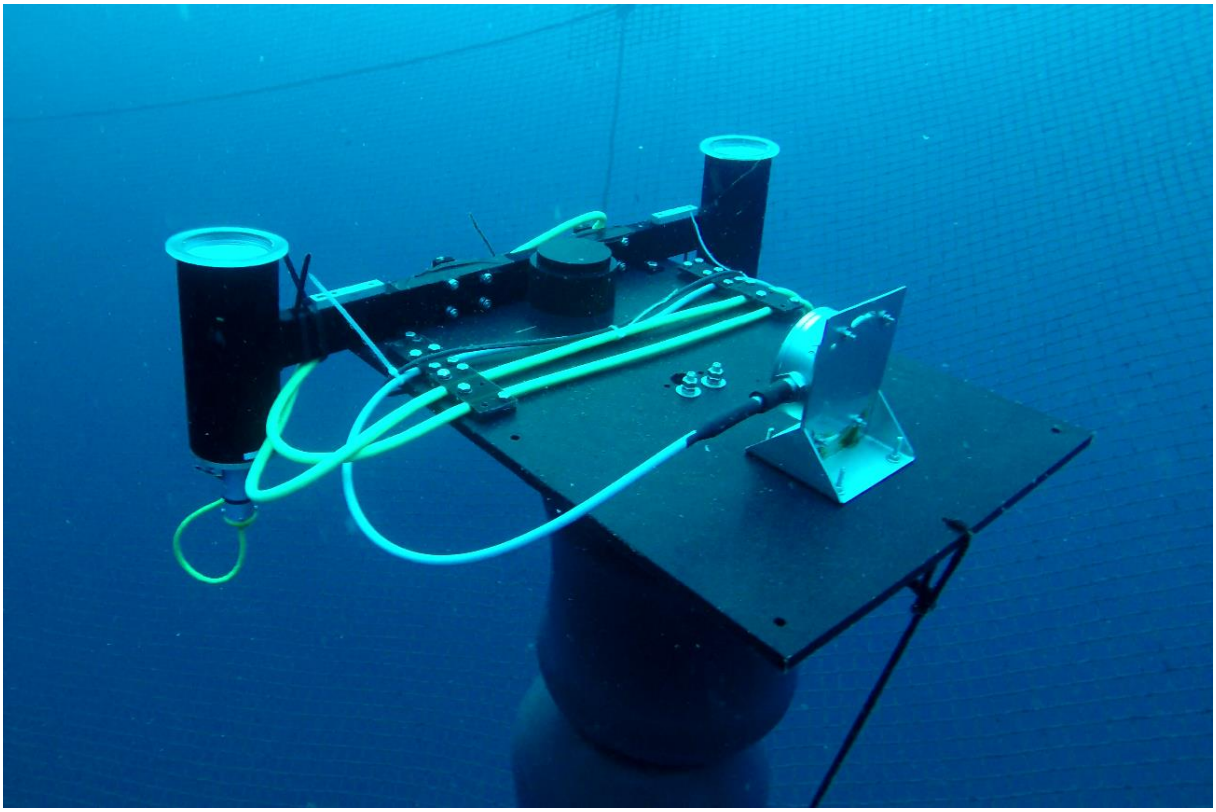

Figure 2. Sensors platform installed in the Grup Balfegó facilities

1.1.2. Logging Subsystem

The logging subsystem is composed of the following elements:

- Battery
- Solar panel
- Logging computer
- Satellite communication (Iridium)
- 4G and Wi-Fi communications
- Underwater connector and cables

The battery and solar panel provide the system with an average time of energy autonomy of 5 hours a day from June to October and 3 hours a day from October to January. Iridium communications enable remote on/off switching and 4G communications allows the cloud storage of the recordings. Figure 3 shows an image of the logging subsystem installed in the Grup Balfegó facilities. The logging subsystem has been designed and built in collaboration with Zunibal S.L.

Figure 3. Logging subsystem installed in the Grup Balfegó facilities, designed and built in collaboration with Zunibal S.L.

1.1.3. Calibration of the system

The stereoscopic system, the acoustic sensors and the relative position and orientation between them were calibrated prior to the installation in the Grup Balfegó facilities.

In the case of the stereoscopic cameras, images were acquired in a swimming pool with 12x6x2 meters. A 1.40 x 1.10 m checkerboard pattern was guided from -45° to 45° with respect to the optical axis and moved between 1 and 10 m away from the cameras. The MATLAB Stereo Calibration Application was used to estimate the calibration parameters. In the case of the acoustic sensor, an on-axis calibration was carried out using a 38.1 tungsten carbide calibration sphere for a 120 kHz acoustic system in a tank containing seawater at IEO (Spanish Oceanographic Institute) facilities in Mazarrón (Spain). To deduce the relative position and orientation between acoustic and optical devices and deal with experimental assembly inaccuracies, a coarse extrinsic calibration between camera and transducer was carried out in the UPV facilities.

Figure 4, Figure 5 and Figure 6 show pictures taken during the calibration process of the stereoscopic system, the acoustic sensor and the acoustic-optic relative transformation, respectively.

Figure 4. Picture taken during the calibration process of the stereoscopic system.

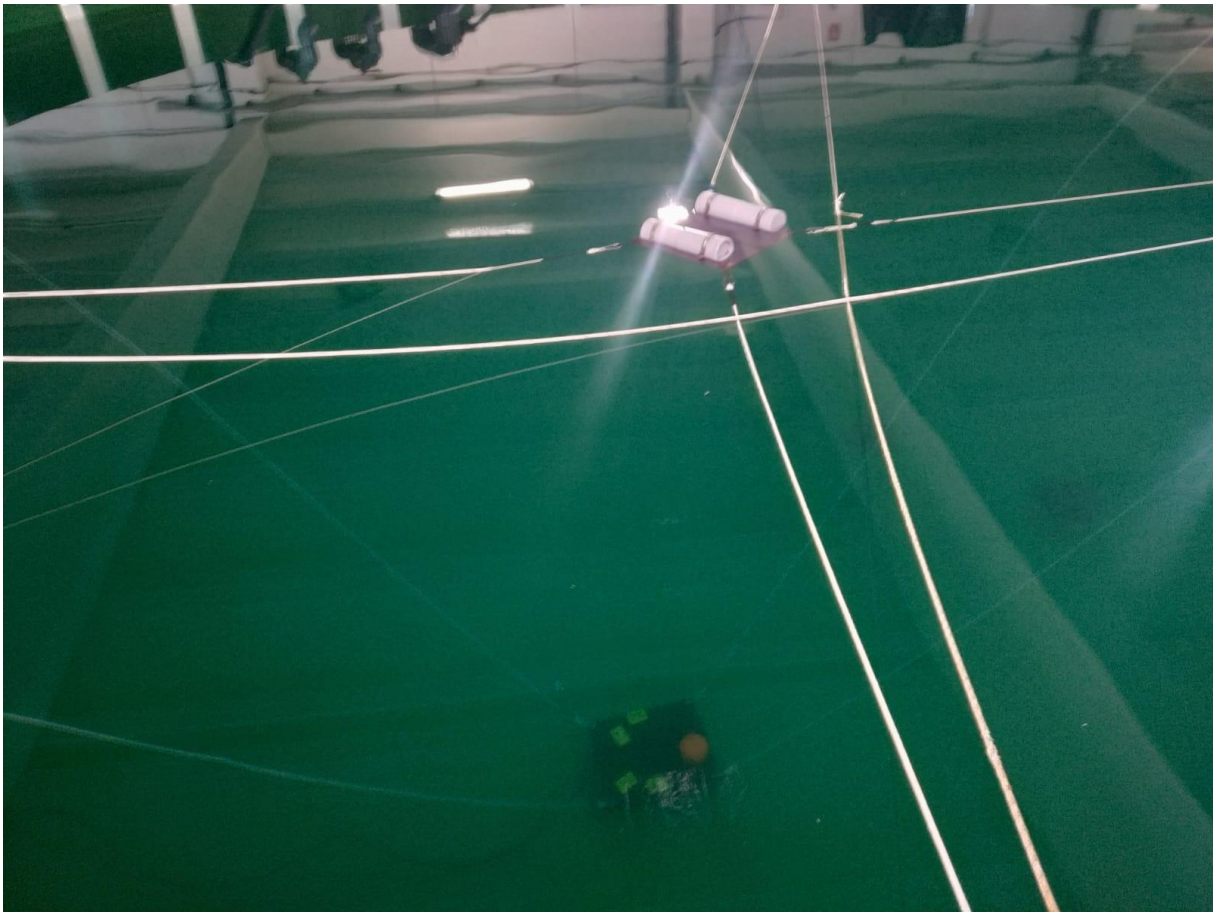

Figure 5. Picture taken during the calibration process of the acoustic sensor.

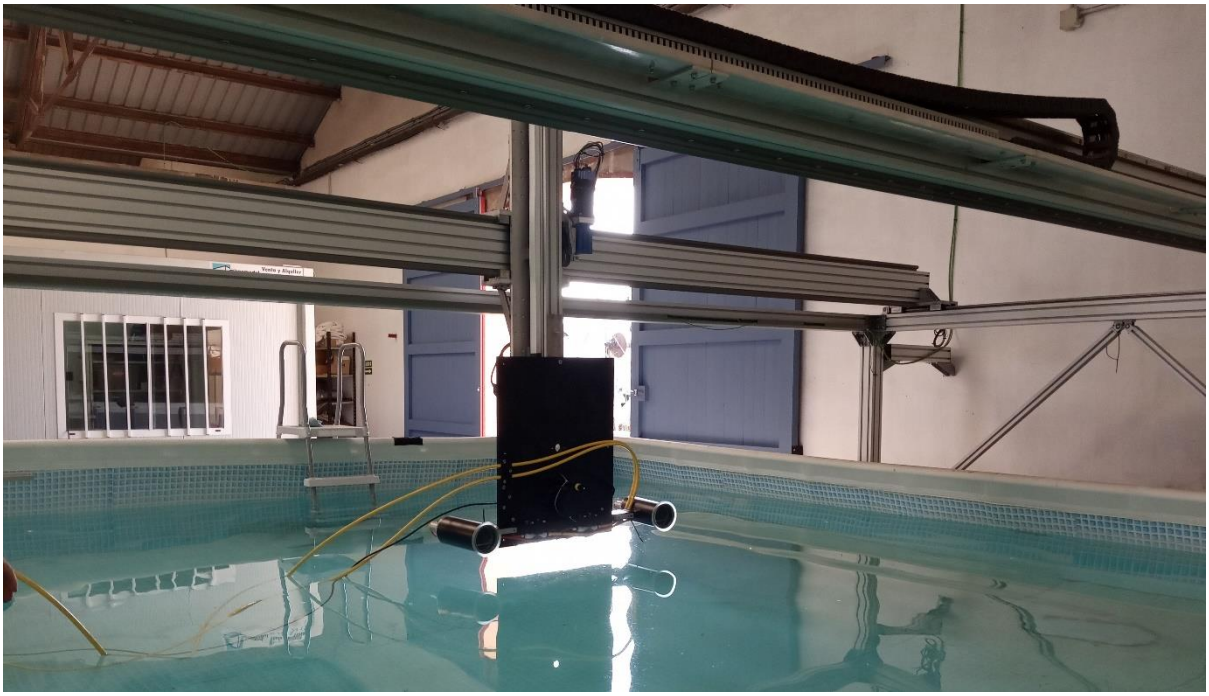

Figure 6. Picture taken during the calibration of the acoustic-optic relative transformation.

1.1.4. Installation of the system

After months of uncertainty due to COVID-19 pandemic, the system was successfully installed in cage #2 in the Grup Balfegó facilities (Spain) in July 28th:

- Figure 7 shows some pictures taken during the installation of the system on board the vessel.
- An image acquired with the stereoscopic system and an acoustic echogram are presented on Figure 8 and Figure 9, respectively.
- A video of the subsea platform in the cage can be watched in this LINK[3].

3https://upvedues-my.sharepoint.com/:v:/g/personal/pamuobe_upv_edu_es/EZkiSo49Sv5Kms__w0YJ0KQBCyYglexseV0KOPsH0i-Rkg?e=ZxDN9k

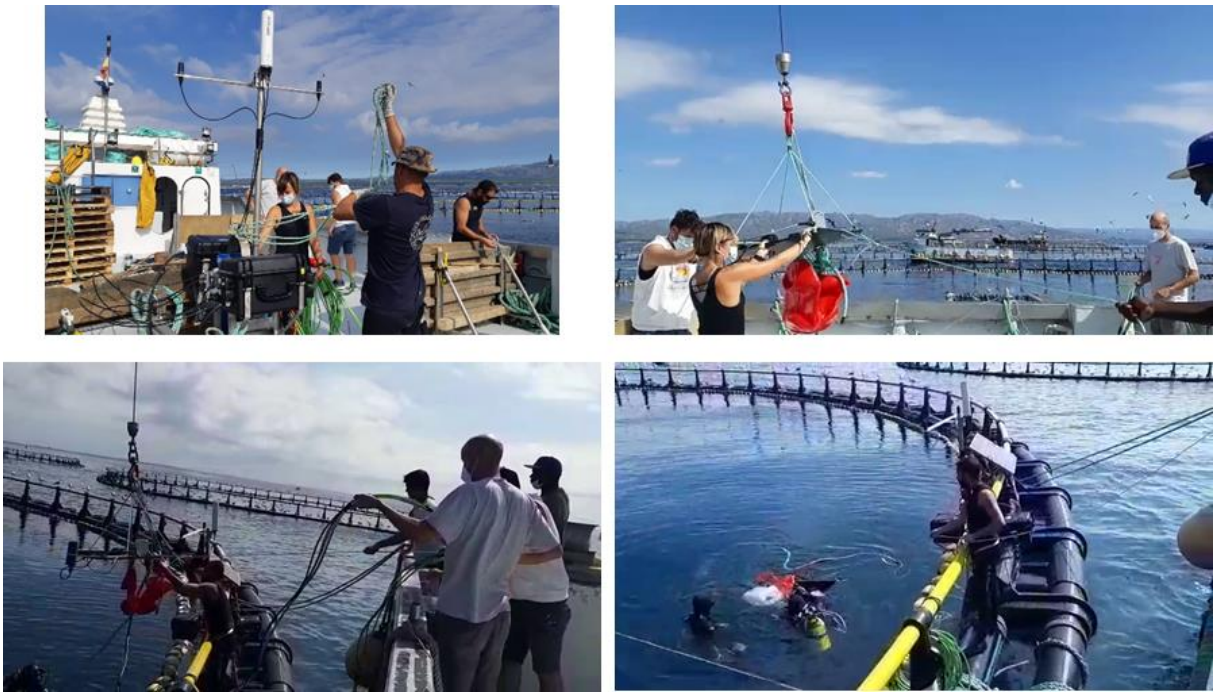

Figure 7. Picture taken during the installation of the system in the Grup Balfegó facilities.

Figure 8. Stereoscopic image acquired with the monitoring system at Grup Balfegó facilities on July 28th.

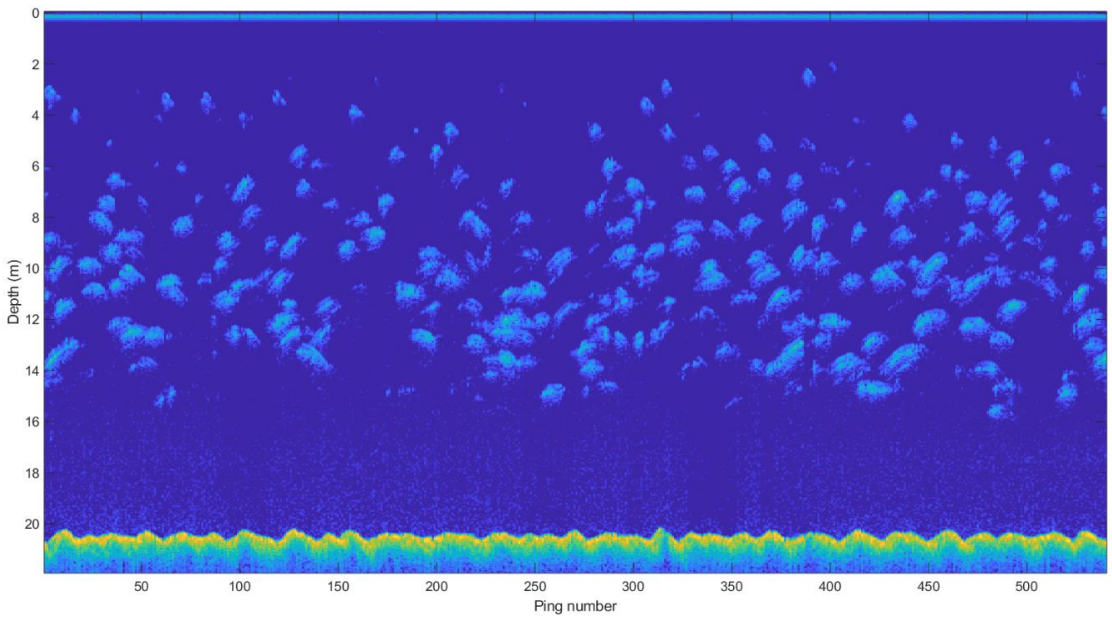

Figure 9. Acoustic echogram acquired with the monitoring system at Grup Balfegó facilities on July 28th.

1.2 Computer vision algorithms for fish width and length estimation

The computer vision algorithms involved in the process of fish sizing are summarized in Figure 10, whereas the image processing steps are depicted in Figure 11. Image segmentation was implemented using local thresholding (Petrou and Petrou, 2011), a region-based technique for extracting compact regions (blobs) on each video frame, and morphological operations. The segmented blobs are geometrically characterized and sifted using shape (aspect ratio), pixel density and dimensional filters. An edge detection algorithm is then applied and a minimization algorithm is used to fit a deformable tuna model. The results for left and right videos, obtained separately, are merged to calculate fish sizes. The image plane information is transformed to 3D measurements using the calibration parameters of the stereoscopic vision system and 3D triangulation. The visual tracking allows us to obtain reliable size measurements based on the repetition of several measurements of the same fish. This visual tracking is based on the fact that once fish are appropriately identified in the video frames and tuna models are fitted to their silhouettes, measurements are considered to belong to the same fish when silhouette models overlap in neighboring video frames and have similar lengths and swimming directions. Fish measurements are computed as the median of all repetitions. An example of the visual tracking can be seen in Figure 12, where one fish is identified and measured 10 times (in 10 almost consecutive frames). See (Atienza-Vanacloig et al., 2016), (P. Muñoz-Benavent et al., 2018a), (P. Muñoz-Benavent et al., 2018b) and (P. Muñoz-Benavent et al., 2020) for further details on the computer vision algorithms.

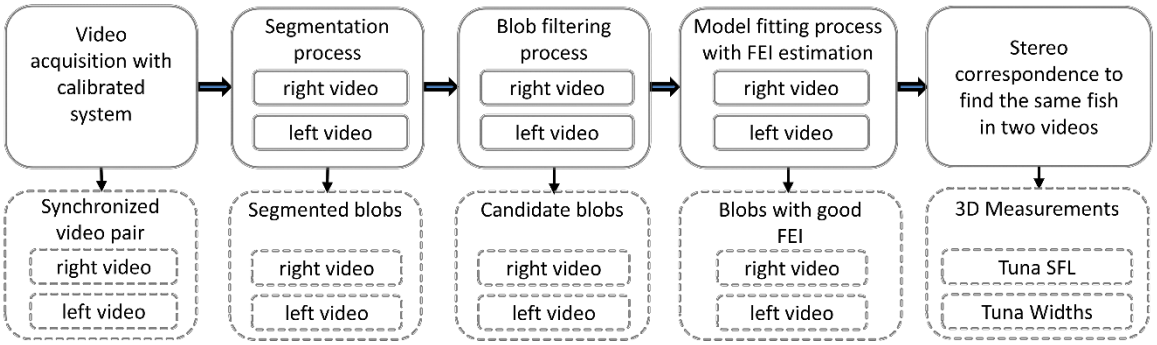

Figure 10. Sequence of processes performed automatically in our proposal, in the first row, and the results of each step, in the second row. Fitting Error Index (FEI) is a coefficient that represents the goodness of the model fitting.

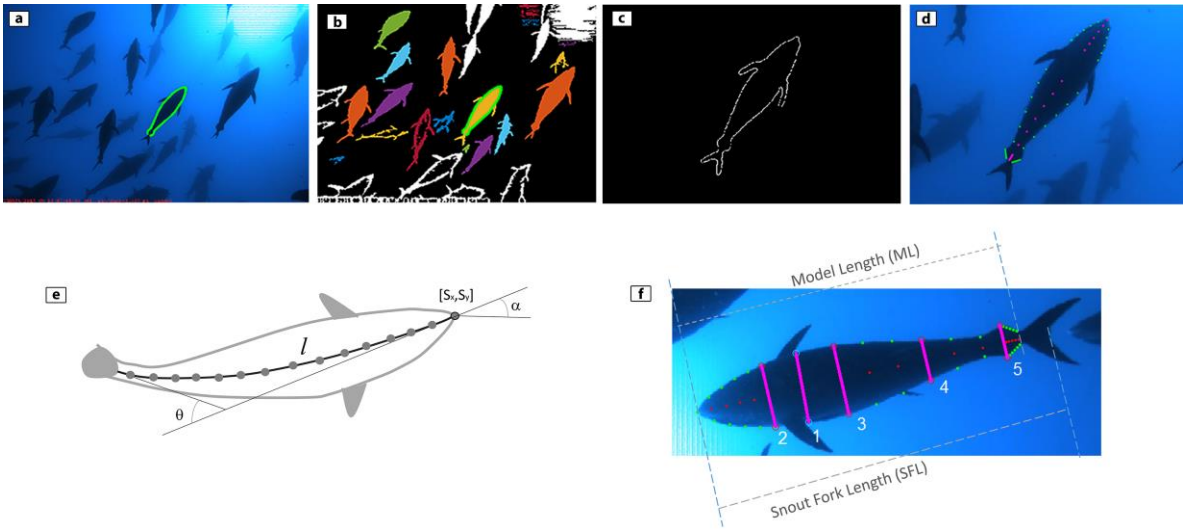

Figure 11. Image processing steps: (a) original image, (b) image segmentation, (c) edge detection, (d) deformable model fitting, (e) deformable tuna model, (f) graphical representation of the Model Length (ML), Snout Fork Length (SFL) and the five widths defined to study the fattening evolution.

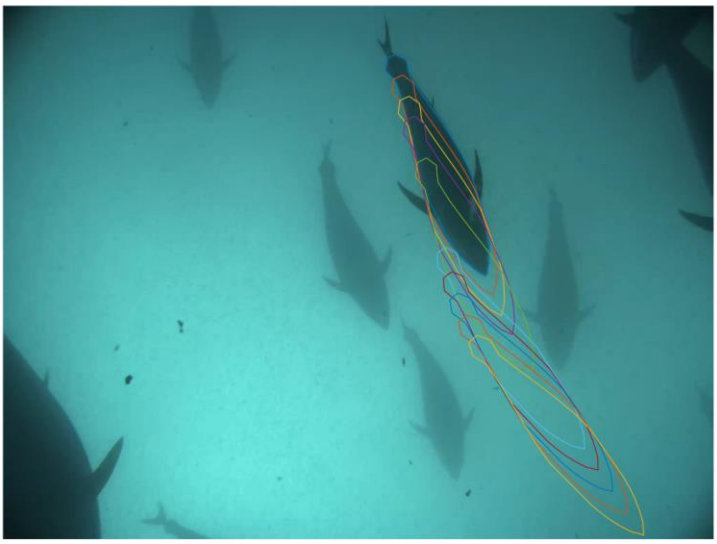

Figure 12. Fish tracking in video frames

1.3 Acoustic algorithms for tuna height estimation

To obtain the acoustic height, acoustic data were previously processed using the automatic algorithm shown in Figure 13. Firstly, the echogram was transformed into a binary image using a threshold level. In the second step, a sequence of morphological operations was applied: thickening to provide traces that are more compact, opening to remove protrusions (noise), breaking weak connections, and closing to smooth out contours and fill small holes. Then, the traces were geometrically characterized and filtered. The next step consists of acoustic properties analysis to select good quality traces. Finally, maximum TS (Target Strength) was analyzed and isolated traces were storage. As a result of the acoustic data processing, a collection of traces characterized by their shape and the distance to the transducer were obtained.

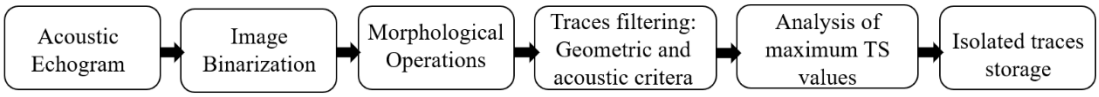

Figure 13. Acoustic data processing performed automatically.

Acoustic height has been calculated from isolated traces (Figure 14a). First, the ping with the maximum acoustic value in the trace was found. Then, acoustic energy of all the bins of this ping were evaluated (Figure 14b). Finally, the beginning and end of trace in this ping were detected (red points Figure 14a) and distance between the beginning point and the end point was calculated. This distance was called Acoustic Height.

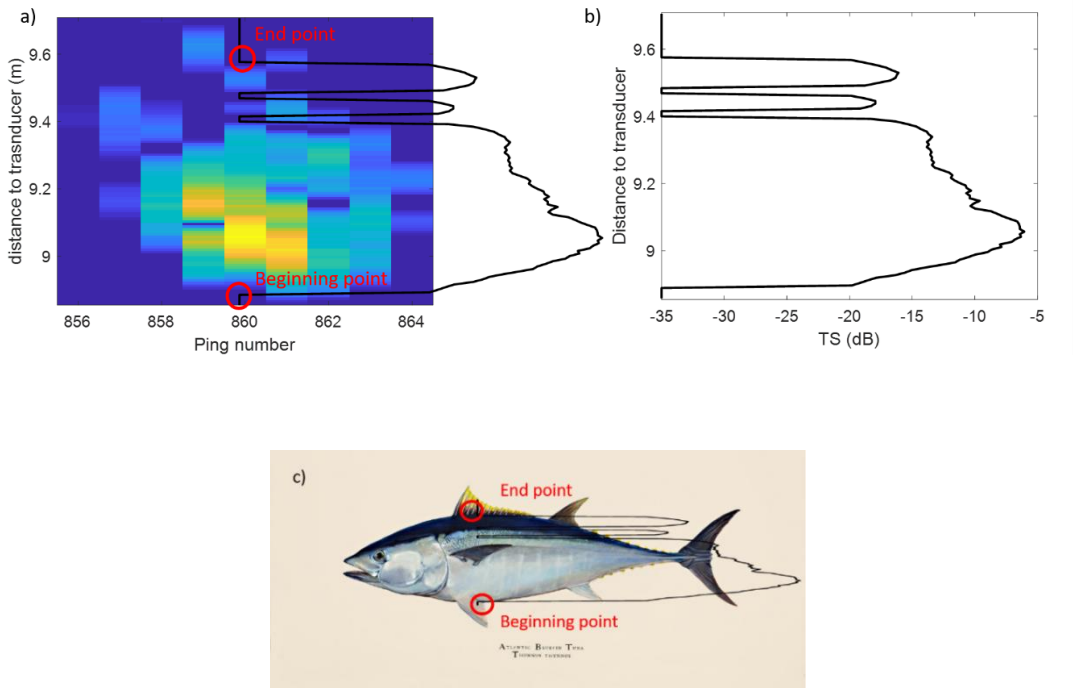

Figure 14. a) Isolated trace image. In red beginning and end points. In black acoustic energy values in the ping that contains maximum energy. b) Acoustic energy in the ping that contains maximum energy (TS). c) Graphical presentation of acoustic height.

In order to obtain biometric information from an individual fish, acoustic and optical data processing were combined (Muñoz-Benavent et al. 2020). As a result, an isolated acoustic trace was associated with a tuna in an image unequivocally. In that way, for the same fish a database was obtained. Fork length, width and swimming tilt were estimated from optical data and height and TS were calculated from acoustic data. To validate acoustic height data, only tuna which swimming tilt was between -5º and +5º were taken into account.

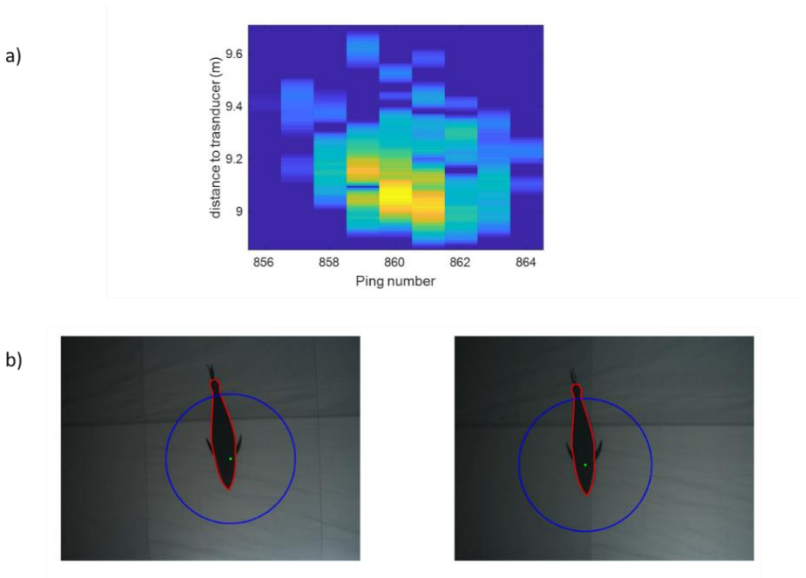

Figure 15. Acoustic trace and corresponding stereoscopic images

The availability of tuna height data is crucial for validating acoustic height. Therefore, tuna height was obtained from videos recorded by AQ1 system during July, September and November. The height of 300 tuna were measured manually and compared with data provided by Grup Balfegó of harvests from March to May in 2012 and 2013. Data from Balfegó harvests were already analyzed in (Puig-Pons et al, 2018) to obtain a relationship between weight and linear dimensions of Bluefin tuna.

1.4 Bhattacharya's method for modal analysis

Taking into account that the fish stock is composed of fish from several different ages, a modal analysis able to identify the different cohorts should be done prior to analyze the evolution of SFL and width. The modal analysis presented in this section is based on the application of the recommendations of "Introduction to tropical fish stock assessment - Part 1: Manual", published by the Food and Agriculture Organization (FAO) of the United Nations in the series "FAO Fisheries Technical Paper". In particular, the Bhattacharya's (1967) method is applied using FiSAT II (FAO-ICLARM Fish Stock Assessment Tools) software, which consists basically of separating normal distributions, each representing a cohort of fish, from the overall distribution. The measurements using the F12 system (July and August) have been omitted, because they are still under analysis.

In spite objective criteria exist to perform the analyses in a proper and standardized way, FiSAT II software allows the operator to decide on the selection of the points which define each modal group, and Bhattacharya's method is sensitive to such selection. So, different results could be obtained depending on the operator decisions. Consequently, to get as much reliable and coherent results, strict criteria for carrying out the analyses were set under the supervision of an expert in fish growth with a deep knowledge of the use of FiSAT software (GBYP coordinator). Finally, the following criteria were applied, which provided results coherent with the existing knowledge on BFT growth:

- Each cohort is defined with as many points as possible located over a descendant straight line. The minimum number of points should be three for the real and well-represented subcohorts. Sometimes, when we have isolated specimens, we have only two points, which we can select to prevent that these specimens are wrongly included in adjacent cohorts.
- SI values (separation index between successive cohorts) should be at least two. In spite, slightly lower values can be admitted between older cohorts.
- SD value should always fall in the range 3.9 to 7 (considering background information about the variability within annual cohorts)
- The number of specimens within each identified cohort should be around 30 or more, since with lower numbers it is difficult to characterize properly the "normal" distributions.

Prior to applying the method, length-frequency data are pre-processed with different class intervals (2, 3, 5) and smoothing options (running average over 3 classes and running average over 5 classes). From these preliminary analyses it was concluded that the best option to characterize annual cohorts was to use a bin of 3 cm and apply a 3 and running average over 3 classes to smooth the data, since larger bins tend to mix several annual cohorts within the same modal group. So, the modal analysis presented in the Results section uses these pre-processing options.

2. Analysis

2.1 Quantification of the SFL measurement error

The visual tracking described in Section 1.2 allows us to perform a study for the quantification of the relative

error associated to our automatic ventral measurements. For fish measured more than one time, the relative error e is defined as the error of each individual measurement with respect to the median of all measurements of the same fish:

$$e_i(\%) = \frac{(SFL_i - \widetilde{SFL})}{\widetilde{SFL}} \cdot 100$$

and the mean relative error $\tilde{e}$ is defined as follows:

$$\tilde{e}(\%) = \frac{\sum_{i=1}^{n} |e_i|}{n}$$

where n is the number of times a fish is measured.

The SFL measurements obtained with the automatic system are grouped in the following day-consecutive periods for the study of the measurement error:

- From September 23rd 2020 to September 30th 2020.
- From October 10th 2020 to October 13th 2020.
- From October 30th 2020 to November 3rd 2020.
- From December 6th 2020 to December 8th 2020.
- From December 13th 2020 to December 18th 2020.
- From March 24th 2021 to March 26th 2021.

To guarantee a high accuracy of the automatic system, only fish that have been measured more than 3 times are considered. In Figure 16, the mean relative error for the different periods is shown. For each box in the boxplot, the bottom side of the central rectangle represents the 25th percentile, whereas the upper side represents the 75th percentile. The red segment inside the rectangle shows the median error. Therefore, it can be seen that the median of the mean relative error is around 0.5% and the 75% of the fish are measured with a mean relative error lower than 0.8% for the periods up to DEC 15-18. They are a bit higher in MAR 24-26 because the lenses used in the AQ1 system have higher radial distortion.

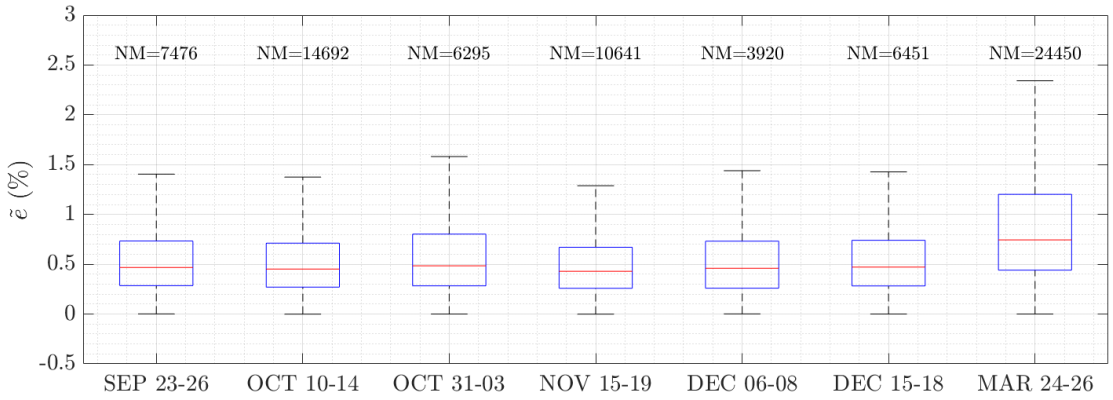

Figure 16. Mean relative error $\tilde{e}$ of fish measured more than 3 times for the different periods. NM: number of measurements.

Another factor to take into consideration is the distance at which the fish are measured. As shown in Figure 17, the relative errors increase with the distance, as expected, since the same deviation in pixels leads to higher deviations in centimeters at higher distances. However, 75% of the measurements (percentile 75th) have an

error below 2% at all distances up to 10 meters. Only SEP and MAR are displayed, but the results are similar to all periods.

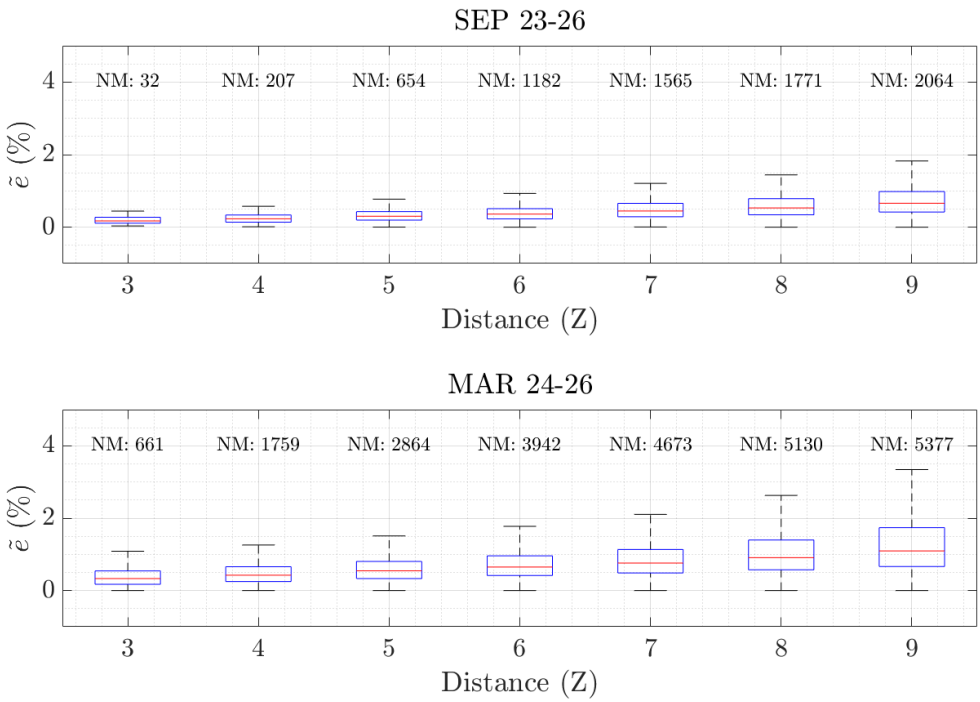

Figure 17. Mean relative error $\tilde{e}$ depending on the distance to the fish.
NM: number of measurements.

We consider that the accuracy of the proposed approach is validated with these results. Even though, to be more accurate in the length estimation, only fish that are measured more than 3 times and that have a relative error lower than 1.5% will be considered.

2.2 Tuna height measurements

Data analyzed in this section have been acquired in July, September and November. These videos were processed with the AQ1 software. Each fish was measured 3 times and length and height averages were calculated. Then, the mean height value of tuna which length was between SFL and SFL+5 cm was calculated, for different SFL values. In Table 1, tuna height for every month is shown. Moreover, mean value for three months are presented. In the same way, data of harvests from March to May in 2012 and 2013 were grouped and compared with AQ1 mean height in Table 1.

When comparing data from harvests with AQ1 data a strong relationship is found. Statistics parameters are presented in Table 2. T-test results show that non-difference between the mean of the two samples exists. An F-Test is run to compare the variances of the two samples. The confidence interval for the ratio of the variances in this case extends from 0,482013 to 2,43976. Since the interval contains the value 1, there is not a statistically significant difference between the standard deviations of the two samples at the 95,0% confidence level. In the same way, a Mann-Whitney W-test to compare the medians of the two samples is done. This test is constructed by combining the two samples, sorting the data from smallest to largest, and comparing the average ranks of the two samples in the combined data. Since the P-value is 0,843 there is not a statistically significant difference between the medians at the 95,0% confidence level. Moreover, a Kolmogorov-Smirnov test to compare the distributions of the two samples. This test is performed by computing the maximum distance between the

cumulative distributions of the two samples. In this case, the maximum distance is 0,0938462, which is shown in Figure 18. As a result of Kolmogorov-Smirnov test a P- value of 0.99 was obtained, it means that there is not a statistically significant difference between the two distributions at the 95,0% confidence level. Finally, values of Standardized skewness and Standardized kurtosis between -2 and 2 indicate that two distributions are normal. This fact validates all tests performed.

	HEIGHT (cm)				
SFL (cm)	AQ1 JUL	AQ1 SEP	AQ1 NOV	AQ1 Mean	Balfegó harvests MAR-MAY 2012-2013
140	41			41	
145	41			41	40
150	42			42	43
155	46			46	43
160	47	42		45	43
165	46	46	48	46	45
170	48	49	51	49	46
1.75	49	50	52	51	48
1.80	51	49	55	52	49
185	51	54	55	54	51
190	54	53	56	54	52
195	58	54	57	56	53
200	57	56	57	56	55
205	58	58	61	59	57
210	61	58	60	60	59
215	62	61	60	61	60
220	62	62	62	62	61
225	64	63	63	63	62
230	65	65	63	64	63
235	67	66	64	66	66
240	67	67	68	67	67
245	70	66	69	68	67
250	71	70	70	70	69
255	71	71	73	72	71
260		71	74	72	72
265	71	69	71	70	74

Table 1. Tuna height measured in AQ1 videos and in harvests in Grup Balfegó from March to May in 2012 and 2013.

	H_Balfego	**H_AQ1**
Count	25	26
Average	56,6	57,2
Standard deviation	10,4	10.0
Coefficient of variation	18,3%	17,5%
Minimum	40	41
Maximum	74	72
Range	34	31
Standardized skewness	0,072	-0,30
Standardized kurtosis	-1,29	-1,23

Table 2. Statistics parameters comparing height from harvests (H_Balfego) with height measured with the AQ1 system (H_AQ1).

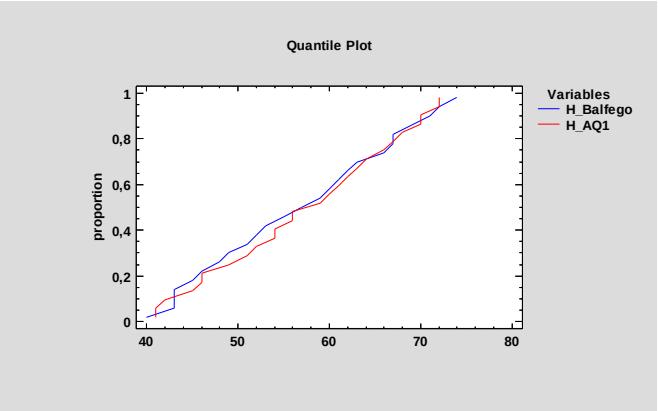

Figure 18. Estimated quantiles of the height from harvests (H_Balfego) and the height measured with the AQ1 system (H_AQ1). If the distributions from which the two samples come are similar, the two curves should be close together.

Finally, a least-squares fitting was performed considering AQ1 data and harvests data (Figure 19). Thus, we obtained a relationship between the height measured by AQ1 and height measured during harvests. A correlation coefficient of 0,99. That fact shows that there is a statistically significant relationship between H_Balfego and H_AQ1 and P-value in Anova analysis confirms this point. In Table 2 a fitting parameters resume is shown.

Fitted model: H_Balfego = 0,981586*H_AQ1

Correlation Coefficient	0,99
R-squared	99,9 %
R-squared (adjusted for d.f.)	99,9%
Standard Error of Est.	1,6
Mean absolute error	1,1
Model P-value	>> 0.001

Table 3- Least-squares fitting parameters between height from harvests and height measured with the AQ1 system.

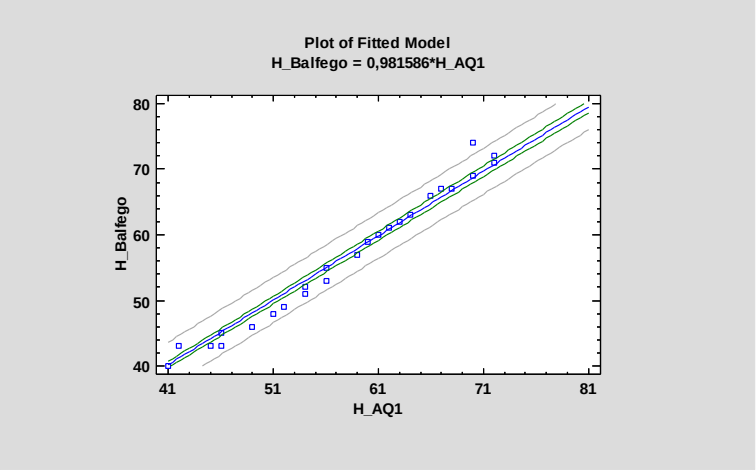

Figure 19. Least-squares model fitting between height from harvests (H_Balfego) and height measured with the AQ1 system (H_AQ1).

Tuna height measurements using AQ1 videos have been compared with tuna height for the same tuna SFL intervals obtained from direct measurements from harvests in the period from March to May in 2012 and 2013. In absence of other ground truthing, data sets showed a strong correlation considering the whole data set from July to November. For this reason, we propose to use AQ1 height measurements to validate height estimation from acoustic data. It must be underlined that tuna height estimated from videos can be referred to the cage population in a particular measurement date, during the fattening process, whilst height from harvests mixes data from different dates during the production season, and it can be affected by different fattening levels. How the fattening process affects tuna height is being investigated.

2.3 Acoustic height measurements

In the same way as tuna height measurements, acoustic and optical data combination were length grouped in 5 cm intervals to compare with AQ1 height measurements. Smaller groups with less than 50 samples were not considered. To see if there is a relationship between tuna height and acoustic height a least squares adjustment was performed. Result is showed in Figure 20. The equation of the fitted model is:

$$H\_AQ1\_mean = -6.54394 + 0.878759*H\_acoustic$$

Since the P-value obtained is less than 0.05, there is a statistically significant relationship between AQ1 height and acoustic height at the 95.0% confidence level. The coefficient of determination, R2, is equal to 0.95, and therefore the model provides a statistically significant explanation (the model as fitted explains 95% of the variability in H_AQ1_mean). The correlation coefficient equals 0.97, indicating a relatively strong relationship between the variables. The standard error of the estimate is 1.5 cm and the mean absolute error obtained is 1.2 cm.

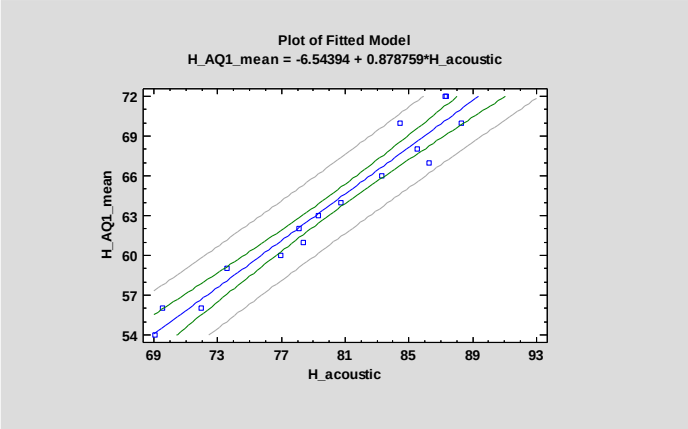

Figure 20. Least-squares model fitting between acoustic height (H_acoustic) and height measured with the AQ1 system (H_AQ1_mean)

In order to evaluate the predictive capability of model a comparison between AQ1 height and results obtained using the fitted model was performed. Statistic parameters are showed in Table 4. A mean comparison using t -test reveal that there is not a statistically significant difference between the means of the two samples at the 95.0% confidence level (confidence interval extends from -7.78114 to 3.08618). In the same way an F-test to compare the variances of the two parameters was done. That test indicates that no significant difference between the standard deviations of the two samples at the 95.0% confidence level exists. A Mann-Whitney W-test is

used to compare the medians. In this case, the P-value is 0.28 (greater than 0.05). It can therefore be concluded that there is not a statistically significant difference between the medians at the 95.0% confidence level. Finally, a Kolmogorov-Smirnov test is performed by computing the maximum distance between the cumulative distributions of the two variables. In this case, the maximum distance is 0.168269 and the P-value is 0.81, it means that there is not a statistically significant difference between the two distributions at the 95.0% confidence level. Table 4 shows the standardized skewness and standardized kurtosis values. Both are within the expected range (-2 to 2) thus the two variables present normal distributions. This fact validates comparison tests.

	H_AQ1_mean	**H_acoustic**
Count	26	32
Average	57.2	59.5
Median	57.5	61.6
Variance	99.8	110.1
Standard deviation	10	10.5
Coefficient of variation	17.4%	17.6%
Standard error	1.95	1.85
Minimum	41.0	31.3
Maximum	72.0	73.7
Range	31.0	42.4
Standardized skewness	-0.30	-1.40
Standardized kurtosis	-1.23	-0.12

Table 4- Statistical parameters comparing acoustic height (H_acoustic) and height measured with the AQ1 system (H_AQ1_mean).

3. Results and conclusions

3.1 SFL evolution

The recordings are grouped in the following day-consecutive periods:

- From September 23rd 2020 to September 30th 2020.
- From October 10th 2020 to October 13th 2020.
- From October 30th 2020 to November 3rd 2020.
- From December 6th 2020 to December 8th 2020.
- From December 13th 2020 to December 18th 2020.
- From March 24th 2021 to March 26th 2021.
- From May 5th 2021 to May 7th 2021.
- From May 21st 2021 to May 23rd 2021.

Taking into account that the fish stock is composed of fish from several different ages, a modal analysis able to identify the different cohorts should be done prior to analyze the evolution of SFL and width. As a prove, Table 5 shows the mean SFL estimated along time with AQ1 samplings from lateral view and harvests provided by Grup Balfegó. It can be seen that the evolution of mean SFL is inconsistent and it is not representative of a fish population containing fish from different ages and lengths. In fact, as it can be seen in September 2020, the mean SFL depends on the number of samples. It differs 6 cm when the number of samples is 20% or 40% of the population. Moreover, the ground truth seems to differ from the mean length estimated before harvesting (May 2021), although it needs to be confirmed when the non-harvested fish are moved to a new cage in August 2021 and estimated with the AQ1 system. Moreover, Figure 21 shows a boxplot of the evolution of SFL measurements using the automatic UPV system. For each box in the boxplot, the bottom side of the central rectangle represents the 25th percentile, whereas the upper side represents the 75th percentile. The red segment inside the rectangle shows the median error. Therefore, it can be seen that the evolution of the median and percentiles along time are not consistent.

	Jul 2020	Sep 2020 20%	Sep 2020 40%	Nov 2020	Mar 2021	May 2021	Ground truth		
							Harvests	Remaining	Combined
Number of fish	724						645	79	724
Mean SFL (cm)	211	223	217	223	216	219	217	147*	209*

Table 5. Mean SFL (cm) estimated along time with AQ1 samplings from lateral view and harvests provided by Grup Balfegó. *Mean SFL of remaining fish has been estimated using the UPV automatic system, since Grup Balfegó plans to move those fish to a new cage in August 2021.

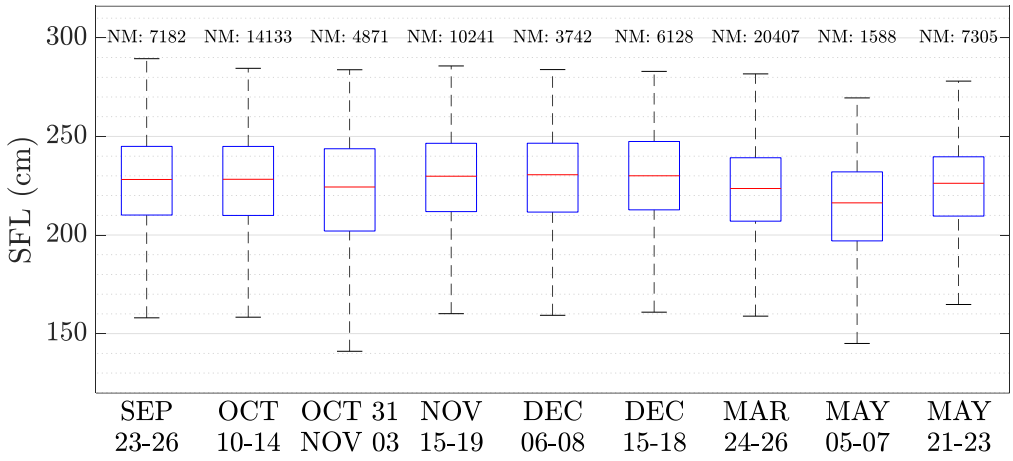

Figure 21. Boxplot of the evolution of SFL measurements using the automatic UPV system.

Once the need of the modal analysis has been proved, the Bhattacharya's method described in Section 1.4 is applied to the SFL measurements obtained with the UPV automatic system. The results of the Bhattacharya analysis can be observed in Table 6. The identification of cohorts and their average SFL are shown in grey, whereas the number of measurements, percentage and number of individuals relative to the number of fish in the cage (724) for each cohort are presented in blue. It can be observed that the percentage of measurements and number of individuals for several cohorts, specifically the first and last ones (smaller and larger specimens) are quite low, most probably because there are in fact very few specimens with those sizes in the monitored cage. Those fishes belong to cohorts different from the well-represented ones, but since they are represented by few individuals, the data cannot be fitted to a modal group. In other cases, it is possible to define a modal group with few specimens, but then the mean lengths of this cohort can be not accurate. Therefore, in spite, they are recorded but they will not be considered for modal progression analyses.

The average SFL of each period and their evolution over time can be observed in Table 7 and Figure 23. The results suggest that growth in length from September to May is approximately between 8 and 18 cm (between 3% and 10%), depending on the fish length. The separation between cohorts decreases as it increases the modal SFL, as expected since the annual growth rates progressively decrease with age. It is also expected that after one year the growth of each cohort be similar to that represented by the distance between consecutive cohorts of the same size range in the initial length distribution. In this case, it is expected that the annual growth, because

of the special conditions in cage, be even higher than in the wild, as has been already demonstrated in juvenile BFT. Our results show that the modal lengths in May 2021 reach already the size of the next cohorts in September 2020.That implies that after one year, each modal SFL could at least reach the next cohort's SFL or a few centimeters more if there is an accelerated growth in cages, as hypothesized.

To corroborate that the cohorts identified in September 2020 correspond to annual cohorts, our modal lengths are compared with the expected body lengths as a function of age according to well-known Von Bertalanffy growth equation applied to BFT (Cort et al., 2014; Landa et al., 2015). As shown in Figure 22, the modal lengths are coherent with the growth equations and they probably represent annual cohorts between 5 and 16 years old.

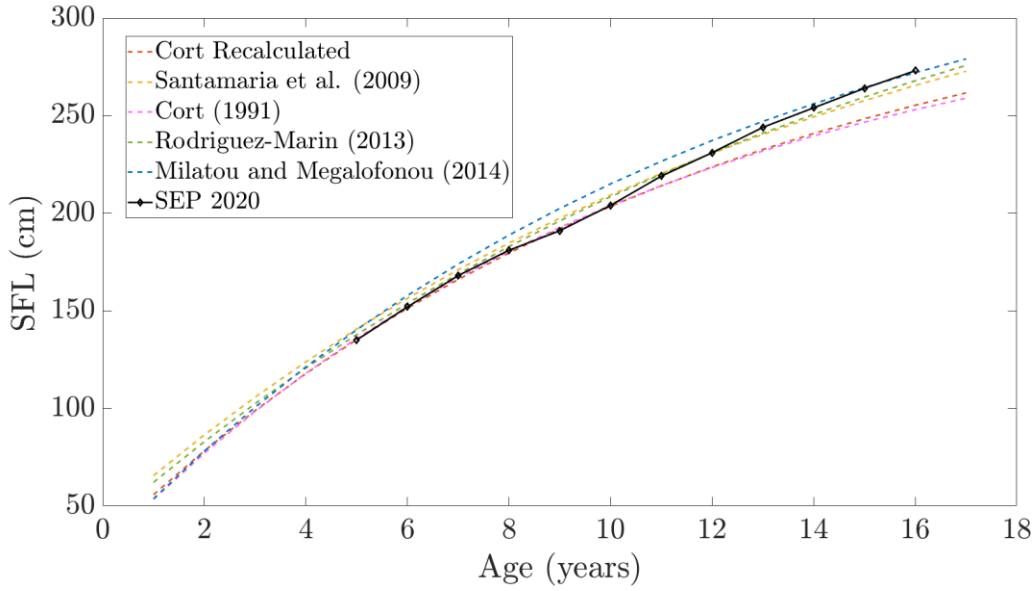

Figure 22. Comparison between cohorts identified in September 2020 with the automatic system and Von Bertalanffy growth curves for BFT of different studies to corroborate that the cohorts identified in September 2020 correspond to annual cohorts.

Cohorts	SEP 23-26			OCT 10-14			OCT 31 - NOV 03			NOV 15-19			DEC 06-08			DEC 15-18			JAN 22-23			FEB 15		
1*	135	24 0.3%	2	139	32 0.2%	2							143	7 0.2%	1	143	13 0.2%	2	143	7 0.2%	1	152		
2*	152	106 1.5%	11	153	311 2.2%	16	154	48 0.9%	6	157	21 0.2%	1	159	114 3%	22	158	123 2%	14	158	91 2.3%	17	167	53 5%	35
3	168	200 3%	20	170	530 4%	27	174	119 2.2%	16	174	156 1.5%	11	176	127 3%	24	175	253 4%	30	174	150 4%	28	179	69 6%	46
4	181	424 6%	42	183	782 5%	40	185	287 5%	38	186	373 4%	26	189	281 7%	53	189	383 6%	45	187	204 5%	37	190	127 12%	84
5	191	467 6%	47	194	1076 7%	54	198	426 8%	56	198	627 6%	44	201	289 8%	55	200	447 7%	52	197	301 8%	55	202	169 15%	112
6	204	734 10%	73	208	1507 10%	76	213	587 11%	78	211	783 8%	55	212	420 11%	80	214	924 15%	108	212	635 16%	117	216	166 15%	110
7	219	1372 19%	137	221	2861 20%	145	224	578 11%	77	223	1199 12%	84	225	763 20%	145	225	1096 18%	128	227	912 23%	168	227	251 23%	166
8	231	1695 23%	170	233	2560 18%	130	236	1191 22%	158	234	1793 17%	126	237	730 19%	139	237	1108 18%	130	240	677 17%	124	238	125 11%	83
9	244	928 13%	93	245	2577 18%	130	248	808 15%	107	246	1987 19%	140	249	608 16%	115	249	1107 18%	130	251	492 12%	90		135 12%	89
10	254	754 10%	75	257	1584 11%	80	259	830 15%	110	256	1685 16%	119	259	351 9%	67	259	510 8%	60	261	383 10%	70	260	6 0.6%	4
11	264	484 7%	48	267	480 3%	24	268	619 11%	82	267	1291 12%	91	269	145 4%	28	269	251 4%	29	271	109 2.7%	20			
12*	273	91 1.3%	9	277	88 0.6%	4				277	431 4%	30												
total samples	7,329			14,538			5,817			10,468			3,851			6,305			1,664			1,101		

Cohorts	MAR 24-26			MAY 5-7			MAY 21-23			HARVESTS	
1*	143	83 0.4%	3	146	34 2.1%	15	148	58 0.8%	6		
2*	158	431 2.1%	15	159	63 4%	28	161	163 2.2%	16	161	7 1%
3	176	1072 5%	37	176	126 8%	56	176	318 4%	31	176	55 8%
4	189	1692 8%	59	191	258 16%	115	191	607 8%	59	188	63 10%
5	201	2015 10%	70	206	338 21%	151	206	1023 14%	99	204	128 20%
6	214	3625 17%	126	219	175 11%	78	222	2330 31%	226	223	221 34%
7	227	5849 28%	204	232	318 20%	142	237	1976 26%	191	240	137 21%
8	242	3922 19%	137	243	207 13%	93					
9	254	1386 7%	48	253	86 5%	38	253	945 13%	92	253	37 6%
10	262	708 3%	25	262	24 1.5%	11	265	78 1.0%	8	266	6 1%
11	271	107 0.5%	4				272	18 0.2%	2		
12*											
total samples	20,942			1,629			7,518			645	

Table 6. Identification of cohorts resulting from Bhattacharya's method for different periods from September to May with the automatic system from the ventral view. In grey and white, average SFL (cm); in blue, number of measurements, percentage and number of individuals according to the number of fish in the cage (724) for each cohort. *Cohorts with few specimens.

Cohorts	SEP 23-26	OCT 10-14	OCT 31 - NOV 03	NOV 15-19	DEC 06-08	DEC 13-18	JAN 21-22	FEB 15	MAR 24-26	MAY 05-07	MAY 21-23	HARVESTS	SEP 2020 MAY 2021
1*	135	139			143	143	143	152	143	146	148		+13 (+10%)
2*	152	153	154	157	159	158	158	167	158	159	161	161	+9 (+6%)
3	168	170	174	174	176	175	174	179	176	176	176	176	+8 (+5%)
4	181	183	185	186	189	189	187	190	189	191	191	188	+10 (+6%)
5	191	194	198	198	201	200	197	202	201	206	206	204	+15 (+8%)
6	204	208	213	211	212	214	212	216	214	219	222	223	+18 (+9%)
7	219	221	224	223	225	225	227	227	227	232	237	240	+18 (+8%)
8	231	233	236	234	237	237	240	238	242	243			+12 (+5%)
9	244	245	248	246	249	249	251		254	253	253	253	+9 (+4%)
10	254	257	259	256	259	259	261	260	262	262	265	266	+11 (+4%)
11	264	267	268	267	269	269	271		271		272		+8 (+3%)
12*	273	277		277									
# samples	7,329	14,538	5,817	10,468	3,851	6,305	1,664	1,101	20,942	1,629	7,518	645	

Table 7. Identification of cohorts and average SFL resulting from Bhattacharya's method and number of samples per period. Length increase in last column. *Cohorts with few specimens.

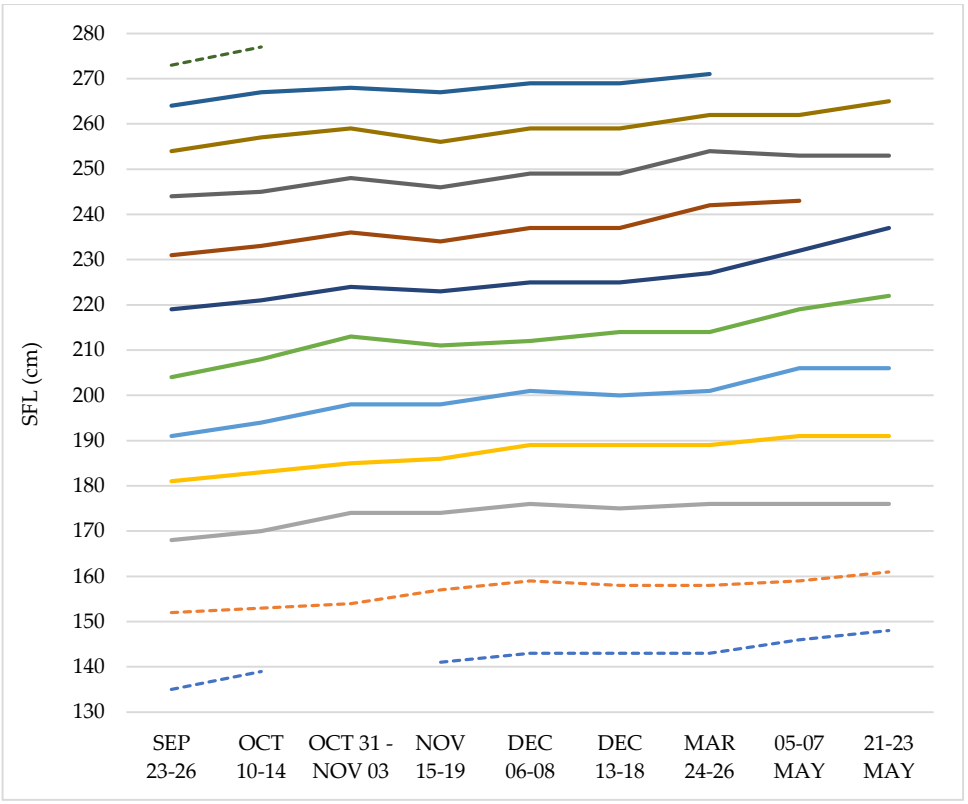

Figure 23. Identification of cohorts and evolution of average SFL resulting from Bhattacharya's method. Cohorts with few specimens represented in dashed-lines.

3.2 Maximum width evolution

As it can be observed in Figure 24, the frequency histogram seems to move to bigger maximum widths (A) from September 2020 to May 2021, i.e., it seems that fish have increased their maximum width an average of 2 cm, but the aforementioned existence of different cohorts, makes it desirable to study widths variations in groups of SFL. Note also that the maximum width increase can be observed in the scatter plots of Figure 25, since in May 2021, the points reach higher values of A for the same SFLs. It can also be observed that the point cloud is narrow in September 2020 and wider in May 2021, what means that there exists more variability of maximum widths, i.e., some of the fish fatten more than others do.

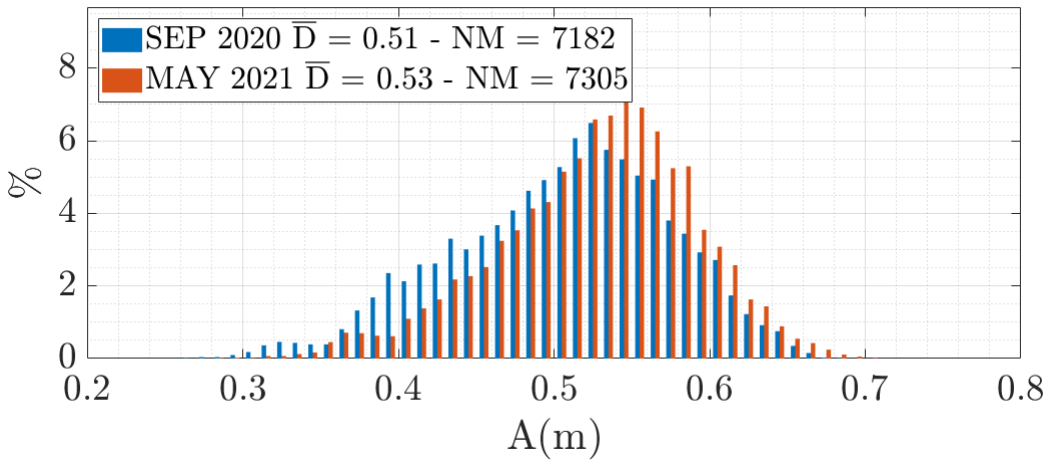

Figure 24. Maximum width (A) frequency histograms for September 2020 and May 2021.

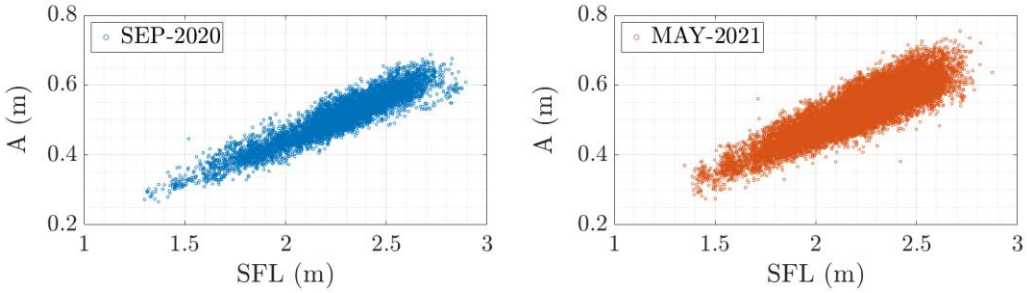

Figure 25. Scatter plots of SFL and maximum width (A) for September 2020 and May 2021.

Considering the existence of fish cohorts, the maximum width has been studied by grouping specimens of similar SFL. Thus, SFL is divided in groups of 10 cm, from 140 to 280 cm, and the average maximum width ($\bar{\mathbf{A}}$) for each group has been calculated. As it can be seen in Table 8 and Figure 26, $\bar{\mathbf{A}}$ increases between 1.2 and 3.0 centimeters (between 2% and 10%), depending on the fish SFL.

	$\bar{\mathbf{A}}$ SEP 2020		$\bar{\mathbf{A}}$ MAY 2021		$\bar{\mathbf{A}}$+
$\mathbf{SFL} \in [\mathbf{140, 150}]$	29.3	45	32.1	36	2.9 (10%)
$\mathbf{SFL} \in [\mathbf{150, 160}]$	31.8	46	33.5	69	1.7 (5%)
$\mathbf{SFL} \in [\mathbf{160, 170}]$	33.3	136	35.3	119	2.0 (6%)
$\mathbf{SFL} \in [\mathbf{170, 180}]$	36.2	223	38.2	232	2.0 (6%)
$\mathbf{SFL} \in [\mathbf{180, 190}]$	37.4	421	40.2	307	2.9 (8%)
$\mathbf{SFL} \in [\mathbf{190, 200}]$	39.5	453	42.5	472	3.0 (8%)
$\mathbf{SFL} \in [\mathbf{200, 210}]$	41.4	450	44.4	619	3.0 (7%)
$\mathbf{SFL} \in [\mathbf{210, 220}]$	44.3	824	47.0	1031	2.8 (6%)
$\mathbf{SFL} \in [\mathbf{220, 230}]$	46.5	1203	49.5	1316	3.0 (6%)
$\mathbf{SFL} \in [\mathbf{230, 240}]$	48.7	1082	51.1	1318	2.4 (5%)
$\mathbf{SFL} \in [\mathbf{240, 250}]$	50.9	972	53.3	938	2.4 (5%)
$\mathbf{SFL} \in [\mathbf{250, 260}]$	53.5	715	55.2	630	1.7 (3%)
$\mathbf{SFL} \in [\mathbf{260, 270}]$	55.4	451	56.6	184	1.2 (2%)
$\mathbf{SFL} \in [\mathbf{270, 280}]$	56.7	110	57.9	33	1.2 (2%)

Table 8. Evolution of average maximum width (A) from September 2020 to May 2021. In grey and white, average maximum widths (A) and their increase (A+) in cm for fish grouped according to their SFL; in blue, number of samples of each cohort.

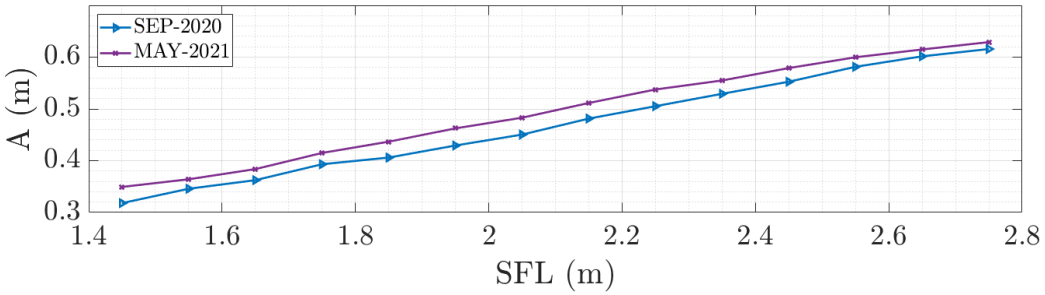

Figure 26. Average maximum width (A) for fish grouped according to their SFL in September 2020 and May 2021.

	$\bar{A}$ SEP 2020		$\bar{A}$ DEC 2020		$\bar{A}$ MAR 2021		$\bar{A}$ MAY 2021	
SFL $\in [140, 150]$	29.3	45	30.2	11	31.0	84	32.1	36
SFL $\in [150, 160]$	31.8	46	32.7	59	33.7	254	33.5	69
SFL $\in [160, 170]$	33.3	136	35.0	38	35.7	264	35.3	119
SFL $\in [170, 180]$	36.2	223	36.4	89	38.2	656	38.2	232
SFL $\in [180, 190]$	37.4	421	38.8	179	40.6	1204	40.2	307
SFL $\in [190, 200]$	39.5	453	40.6	236	42.6	1486	42.5	472
SFL $\in [200, 210]$	41.4	450	42.1	255	44.9	1845	44.4	619
SFL $\in [210, 220]$	44.3	824	44.6	437	47.3	3134	47.0	1031
SFL $\in [220, 230]$	46.5	1203	47.2	536	49.4	3615	49.5	1316
SFL $\in [230, 240]$	48.7	1082	49.7	573	51.6	2986	51.1	1318
SFL $\in [240, 250]$	50.9	972	51.2	570	53.8	2574	53.3	938
SFL $\in [250, 260]$	53.5	715	53.9	454	55.8	1550	55.2	630
SFL $\in [260, 270]$	55.4	451	55.6	233	57.3	650	56.6	184
SFL $\in [270, 280]$	56.7	110	58.4	64	58.5	93	57.9	33

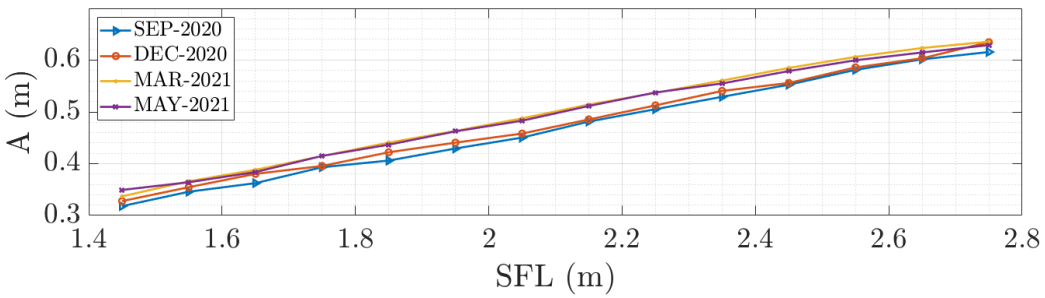

Figure 27. Average maximum width (A) for fish grouped according to their SFL between September 2020 and May 2021.

3.3 Maximum height evolution

According to the results shown in Table 8, maximum width increases between 1 and 3 cm. Similar height rises could be expected. Due to the equipment (single beam echosounder) and setup available (150 µs pulse duration), the associated error of height estimation can be up to over half of pulse length (± 11 cm). For this reason, maximum height evolution could not have been evaluated. However, mean height values could be used to improve weight estimation such as is shown in section 3.5.

3.4 TS vs SFL relationship

Stereoscopic system has to work in a near range where it has good accuracy. TS-SFL correspondences only can be found in a close range to the transducer. This fact causes that acoustic data must be corrected to balance the negative effects due to measurement range. Near field effects in acoustic measurements are well known (Perez-Arjona et al., 2018), to correct them numerical simulations of target strength in the near field of Bluefin tuna are now being carried out.

Once numerical simulations will be completed, corrected TS values will be used to obtain a significant correlation between TS and logarithmic SFL. Moreover, corrected TS could be used to estimate the fish number housed in the cage.

3.5 Biomass estimation

ICCAT proposes the use of the expression proposed in (Deguara et al., 2017) to estimate tuna weight (W) from tuna length (SFL), which fits well during the purse seine fishing season in the Mediterranean:

$$W_{ICCAT} = 2.8684 \cdot 10^{-5} * SFL^{2.907}$$

However, after the fish remains some months in the fattening cages, the weights estimated from SFL measured at harvesting differ from the weights at harvesting, as shown in Figure 28.

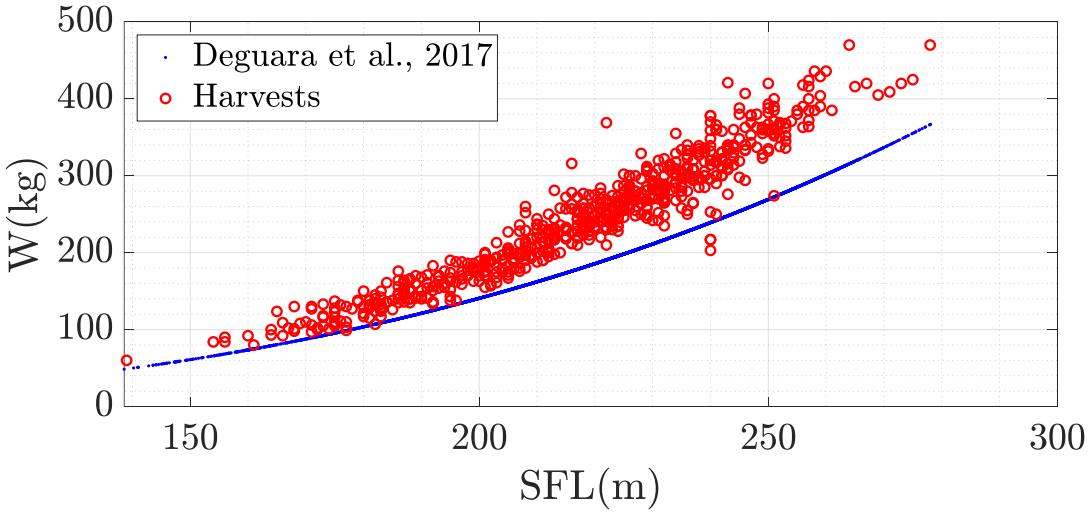

Figure 28. Comparison between SFL-W relationship from (Deguara et al. 2017) and measured weight at harvesting

In (Puig-Pons et al, 2018) relationship between weight and linear dimensions of Bluefin tuna were already analyzed using data from Balfegó harvests. One of the conclusions was that the weight could be better estimated using various dimensions apart from length and proposed the following equations:

$$M1 = 8.05636 \cdot 10^{-5} * SFL^2 * H$$

$$M3 = 7.21719 \cdot 10^{-5} * SFL^{2.07092} * A$$

$$M11 = 1.0775 \cdot 10^{-4} * SFL^{1.67757} * H^{1.26742} * A^{0.091396}$$

Taking into account that the automatic system can deliver length (SFL), maximum width (A) and maximum height (H), the weight of each sample can be estimated using the previous equation. Measurements of the last recordings before harvesting (May 21-23) are plotted together with the weight from harvests and the estimations using SFL-W relationship from (Deguara et al., 2017) in Figure 29. As it can be seen, the weight estimated with M1, M3 and M11 equations from (Puig-Pons et al., 2018) fits well with the measured weights at harvesting. Moreover, as it can be seen in Figure 30, the weights in May 2021 are higher than in September 2020 for the same lengths.

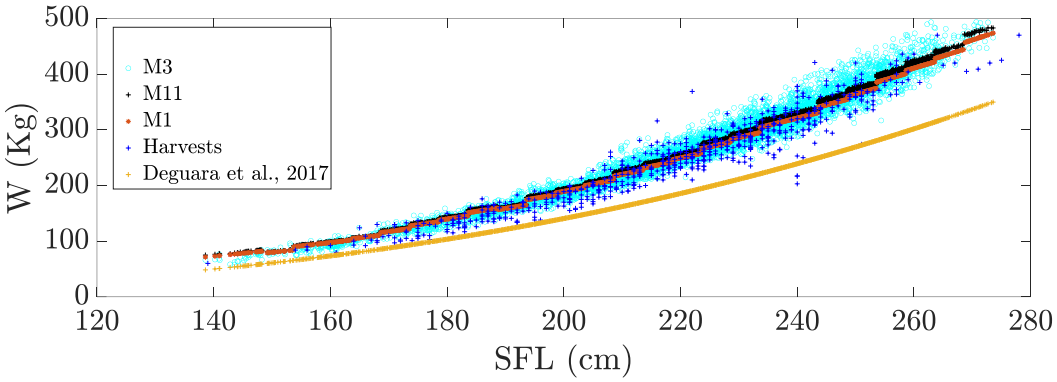

Figure 29. Comparison of estimated weights using SFL-W relationship from (Deguara et al., 2017), using SFL-A-H-W relationships (M3, M11, M1) from (Puig-Pons et al., 2018) and using the measured weights at harvesting

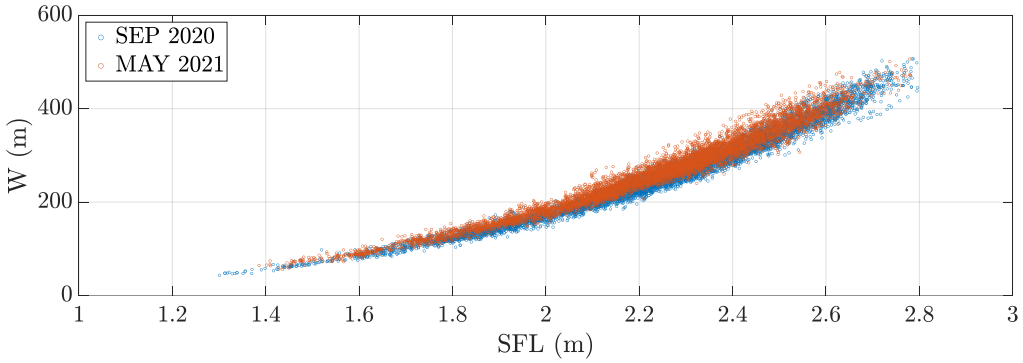

Figure 30. Estimated weight using SFL-A-W relationship (M3) from (Puig-Pons et al., 2018) in September 2020 and May 2021.

The 645 harvested fish have been weighted at harvesting and add up to a total of 158,019 kg, according to the field tokens delivered by Grup Balfegó, and 160,459 kg, according to the report presented by Grup Balfegó. The remaining 79 fish were not harvested and will be transferred to another cage in August 2021. Those fish were recorded with our system and processed using the automatic procedure, which estimated a mean length of 147 cm and a mean maximum width of 31 cm. Applying M3 equation, the mean weight is 69 kg and the biomass of the 79 fish can be considered as 5,441 kg. Thus, we consider that the 724 fish in the cage add up to a total of 163,000-166,000 kg. Total biomass can be estimated from mean SFL by applying SFL-W relationship from (Deguara et al., 2017) and multiplying by the number of fish. In this case, the total biomass is 125,062 kg, which is far from the real biomass because the SFL-W relationship from (Deguara et al., 2017) does not seem to work properly in fattened fish. It could also be estimated using the mean weight deduced with the SFL-A-W relationship from (Puig-Pons et al., 2018) with mean SFL and mean A, which delivers a 10% overestimation, or the mean weight of all the samples, which delivers a 14.8% overestimation.

	Mean SFL (cm)	Mean A (cm)	Mean H (cm)	Mean W (kg)	Number of fish	Biomass (kg)	Remaining Biomass (kg)	Biomass (kg)
Harvests				248.77	645	160,459	5,441	166,582
Harvests from SFL Deguara et al., 2017	217.44			179.34	645	115,677	5,441	121,118 (-27%)
M1	222.61	48.24	62	247.52	724	179,204	0	179,204 (+7.6%)
M3	222.61	48.24		253.14	724	183,273	0	183,273 (+10%)
M11	222.61		62	248.98	724	180,262	0	180,262 (+8.2%)

Table 9. Biomass estimation.

We have to search for the explanation to the overestimation in the weight-frequency distributions (Figure 31). The distributions of harvests and the distribution of the automatic measurements do not have the same profile. Fish with weight within 100 and 250 kg are under-represented in the recordings, causing a bias in the estimation. The causes should be studied in future experiments related to fish behavior and statistics.

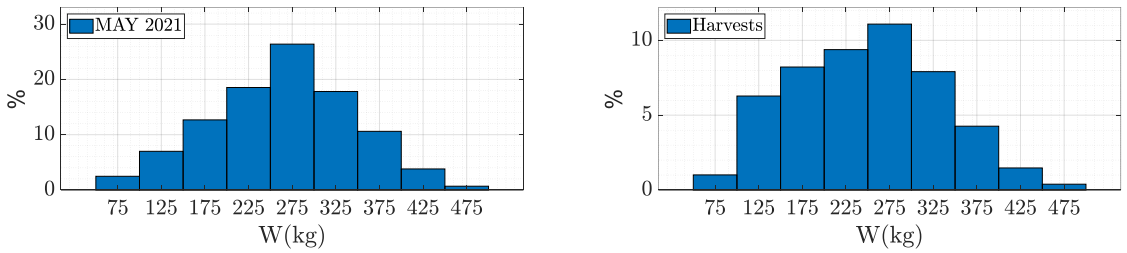

Figure 31. Weight-frequency distribution in May 2021 and in harvests.

According to AQ1 samplings and harvests provided by Grup Balfegó, the biomass estimation along time is presented in Table 10. The biomass evolution is inconsistent, because it is deduced from mean SFL and (Deguara et al., 2017) expression. This expression is only valid during the purse seine fishing season and the mean SFL is not fully representative of a fish population containing fish from different ages and lengths.

	Catch	Jul 2020	Sep 2020	Sep 2020 40%	Nov 2020	Mar 2021	May 2021	Deguara Harvests	Ground truth		
									Harvests	Remaining	Combined
Number of fish	728	724							645	79	724
Mean SFL (cm)	185	211	223	222	223	216	219	217	217	147*	209*
Mean W (kg)	112	164	193	191	193	176	183	178	249	57	228
Biomass (Ton)	**82**	**119**	**140**	**138**	**140**	**127**	**133**	**129**	**161**	**5**	**166**

Table 10. Mean SFL (cm), mean W (in kg) and total biomass (in Tons) estimated along time with AQ1 samplings and harvests provided by Grup Balfegó. *Mean SFL of remaining fish has been estimated using the UPV automatic system, since Grup Balfegó plans to move those fish to a new cage in August 2021.

4. Executive Summary

The present work describes the results obtained with an autonomous monitoring system installed from 28th July 2020 to 23rd May 2021 in a fattening cage in Grup Balfegó (West Mediterranean) containing 724 BFT. The system is able to provide thousands of accurate automatic measurements per day, so the evolution of tuna sizes can be studied in detail thanks to such a great amount of information. The recordings have been grouped in day-consecutive periods along the year. It has been verified that the evolution of the median and percentiles along time cannot be used to estimate growth of a fish population containing fish from different ages and lengths. Instead, a modal analysis able to identify the different cohorts should be done prior to analyze the evolution of length, width and height. The Bhattacharya's method has been applied to the length measurements to identify the cohorts and the results suggest that from September 2020 to May 2021 the growth in length is approximately between 8 and 18 cm (between 3% and 10%) and the growth in maximum width between 1.2 and 3.0 centimeters (between 2% and 10%), depending on the fish length. The acoustic system is also used to estimate the height of the fish to provide a more accurate biomass estimation. Different expressions deduced from slaughtered fish are proposed based on formulae relating weight and dimensions (length, width and height) of Bluefin tuna fattened in captivity. The results confirm that, for tuna fattened in cages, the availability of more than one dimension to estimate weight improves the predictive power of the model and reduces error in the estimate. The proper mechanical robustness, energetic autonomy and communications setup has been achieved thanks to the collaboration of Zunibal S.L in the design and manufacturing of the logging subsystem.

5. Acknowledgements

This work has been carried out under the ICCAT Atlantic-Wide Research Programme for Bluefin Tuna (GBYP), which is funded by the European Union, several ICCAT CPCs, the ICCAT Secretariat, and other entities (see https://www.iccat.int/gbyp/en/overview.asp). The content of this paper does not necessarily reflect ICCAT's point of view or that of any of the other sponsors, who carry no responsibility. In addition, it does not indicate the Commission's future policy in this area.

References

Atienza-Vanacloig, V., Andreu-García, G., López-García, F., Valiente-Gonzólez, J.M., Puig-Pons, V., (2016). Vision-based discrimination of tuna individuals in grow-out cages through a fish bending model. Computers and Electronics in Agriculture 130, 142–150. https://doi.org/10.1016/j.compag.2016.10.009

Cort, José L., Arregui, Igor, Estruch, Vicente D. & Deguara Simeon (2014). Validation of the Growth Equation Applicable to the Eastern Atlantic Bluefin Tuna, Thunnus thynnus (L.), Using Lmax, Tag-Recapture, and First Dorsal Spine Analysis, Reviews in Fisheries Science & Aquaculture, 22:3, 239-255, DOI: 10.1080/23308249.2014.931173.

Girshick R., Donahue J., Darrell T., and J. Malik, (2014) "Rich feature hierarchies for accurate object detection and semantic segmentation," Proc. IEEE Comput. Soc. Conf. Computer Vision and Pattern Recognition, pp. 580–587, 2014.

Deguara, S., Gordoa, A., Cort, J.L., Zarrad, R., Abid, N., Lino, P.G., et al. (2017). Determination of a length-weight equation applicable to Atlantic bluefin tuna (Thunnus thynnus) during the purse seine fishing in the Mediterranean. Collect. Vol. Sci. Pap. ICCAT, 73(7), 2324-2332.

ICCAT (2014). 14-04 Recommendation by ICCAT amending the recommendation 13-07 by ICCAT to establish a multi-annual recovery plan for Bluefin Tuna in the eastern Atlantic and Mediterranean. Compendium Management Recommendations and Resolutions Adopted by ICCAT for Conservation of Atlantic Tunas and Tuna-Like Species, pp. 47–82.

Landa, J., Rodriguez-Marin., E., Luque, P.L., Ruiz, M., Quelle, P. (2015). Growth of bluefin tuna (Thunnus thynnus) in the North-eastern Atlantic and Mediterranean based on back-calculation of dorsal fin spine annuli. Fish. Res., 170, pp. 190-198

LeCun, Y. K., Kavukcuoglu, and C. Farabet (2010) "Convolutional networks and applications in vision," in ISCAS 2010 - 2010 IEEE International Symposium on Circuits and Systems: Nano-Bio Circuit Fabrics and Systems, 2010, pp. 253–256.

Muñoz-Benavent, P., Andreu-García, G., Valiente-González, J.M., Atienza-Vanacloig, V., Puig-Pons, V., Espinosa, V., (2018a). Automatic Bluefin Tuna sizing using a stereoscopic vision system. ICES Journal of Marine Science 75, 390–401. https://doi.org/10.1093/icesjms/fsx151

Muñoz-Benavent, P., Andreu-García, G., Valiente-González, J.M., Atienza-Vanacloig, V., Puig-Pons, V., Espinosa, V., (2018b). Enhanced fish bending model for automatic tuna sizing using computer vision. Computers and Electronics in Agriculture 150, 52–61. https://doi.org/10.1016/j.compag.2018.04.005

Muñoz-Benavent, P.; Puig-Pons, V.; Andreu-García, G.; Espinosa, V.; Atienza-Vanacloig, V.; Pérez-Arjona, I. (2020). Automatic Bluefin Tuna Sizing with a Combined Acoustic and Optical Sensor. Sensors 2020, 20, 5294. https://doi.org/10.3390/s20185294

Pérez-Arjona, I., Godinho, L., and Espinosa, V. 2018. Numerical Simulation of Target Strength Measurements from Near to Far Field of Fish Using the Method of Fundamental Solutions. Acta Acustica united with Acustica, 104(1), 25-38

Phillips, K., Rodriguez, V. B., Harvey, E., Ellis, D., Seager, J., Begg, G., and Hender, J. (2009). Assessing the operational feasibility of stereo-video and evaluating monitoring options for the Southern Bluefin Tuna Fishery ranch sector, Fisheries Research and Development Corporation and Bureau of Rural Sciences (Australia). Report 2008/44, ISBN 978-1-921192-32-6.

Puig-Pons, V.; Estruch, V.D.; Espinosa, V.; De La Gándara, F.; Melich, B.; Cort, J.L. (2018). Relationship between weight and linear dimensions of bluefin tuna (Thunnus thynnus) following fattening on western mediterranean farms. PLoS ONE 2018, 13, e0200406.

Zhang, Y. K. Sohn, R. Villegas, G. Pan, and H. Lee, (2015). "Improving Object Detection With Deep Convolutional Networks via Bayesian Optimization and Structured Prediction," Proc. IEEE Conf. Computer Vision and Pattern Recognition, 2015.